DETERMINATION OF SPALLATION RESIDUES IN THIN TARGET: TOWARD AN HYBRID REACTOR LEAD TARGET SIMULATION

L. Audouin[a] [1], L. Tassan-Got[a], M. Bernas[a], T. Enqvist[b], P. Armbruster[b], J. Benlliure[d], A. Boudard[c], E. Casajeros[d], S. Czajkowski[e], B. Fernandez[c], R. Legrain[c], S. Leray[c], J. Pereira[d], F. Rejmund[a], M.-V. Ricciardi[b], K.-H. Schmidt[b], C. Stéphan[a], J. Taieb[a], C. Volant[c], W. Wlazlo[c].

[a] IPN Orsay, CNRS-IN2P3, 91406 Orsay, France.
[b] GSI, Planckstrasse 1, 64291 Darmstadt, Germany.
[c] DAPNIA-SPhN, CEA Saclay, 91191 Gif-sur-Yvette, France.
[d] University of Santiago de Compostella, 15706 Santiago de Compostella, Spain.
[e] CENBG, CNRS-IN2P3, 33175 Gradignan, France.

Abstract

The production of spallation primary residual nuclei in thin target has been studied by measurement of isotopic yields distributions for several systems. Issues relevant for the design of accelerator-driven systems are presented. Monte-Carlo code abilities to reproduce data are studied in details; it is shown that calculations do not reproduce data in a satisfactory way. Future work orientations leading to an improvement of thin targets calculations and ultimately to a thick target simulation are discussed.

Keywords: *Spallation residues cross-section in thin target; inverse kinematics method ; simulation of ADS spallation target.*

1 Introduction

Among the studies dedicated to nuclear waste management and innovative ways of energy production, the hybrid reactor concept is certainly one of the most promising. An hybrid reactor, also called Accelerator Driven System (ADS), is a subcritical nuclear reactor associated to an external neutron source. In most studies, this neutron source is provided by a high intensity, light particle beam hitting a thick target of heavy material, producing spallation nuclear reactions.

The number and the energy spectra of the neutrons produced in the spallation target is a key point to determine the working conditions of an ADS. Around 30 neutrons per 1 GeV incident proton are expected to escape from a lead target [1]. But there is another key point about the target, which may be problematic in a technological viewpoint: the evolution of the target with time. At least four problems are expected to occur: radiotoxicity of the target material (and maybe neutronic poisoning), corrosion of the target vessel, gaseous emissions, and target heating.

Radiotoxicity, corrosion and target heating are directly related to the spallation residues. The window between the accelerator and the target is also concerned by the residues formed within it, for mechanical (fragilisation of material by atom displacement) and chemicals reasons. Furthermore, isotopic residue distributions provide strong constraint on the spallation calculations, which are obviously needed in order to study all target aspects. For all those reasons, we have undertaken a comprehensive measurement campaign in GSI, aiming at determining full isotopic residues distributions for several spallation thin targets and energies. Experimental method and first results are presented in section 2. In section 3 we discuss simulations codes. In section 4 we summarize the remaining challenges of a complete thick target simulation.

[1] Presenting author - e-mail: audouin@ipno.in2p3.fr

2 Experimental results about spallation residues

Spallation reactions have been studied since the fourty's. The production of residue was studied via radiochemical methods and mass spectrometry of irradiated targets. So, with the exception of a few "protected" fragments, only cumulative mass yields, following β decay chains, have been obtained so far. Recent data cover wide ranges of incident energy and/or targets [2, 3].

2.1 Inverse kinematical method

In order to obtain experimental, isotopic cross sections for residues production, a series of measurements has been undertaken at GSI since 1997. These measurements are based on inverse kinematical method: very heavy ions are accelerated at relativistic energy and imping on a liquid hydrogen target located at the entrance of a fragment separator, the FRS spectrometer [4] (fig. 1). The projectile energy is such that the energy in the center of mass is the same as in direct kinematic (for example a 1 GeV proton projectile on lead is equivalent to a 208 GeV lead on proton).

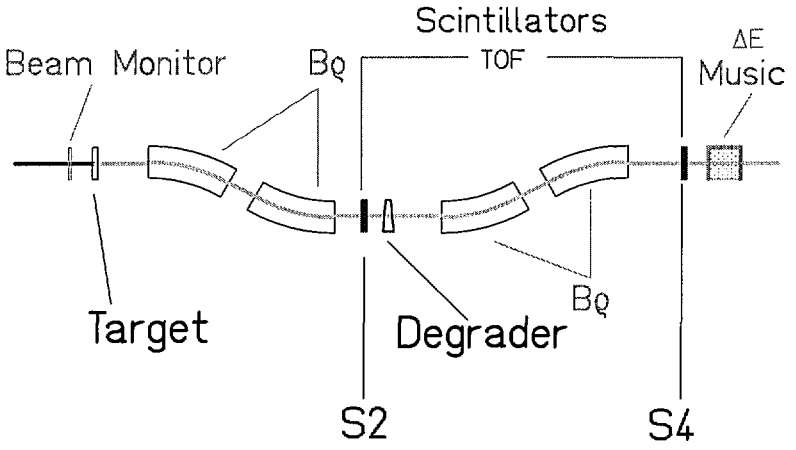

Figure 1: *Schematic drawing of the fragment separator FRS and its detector equipement. The beam monitor measures the incident ions number. Scintillators provide magnetic rigidity and time of flight of the fragment. MUSIC chambers give nuclear charge.*

As the reaction fragments have a velocity close to the projectile velocity, and since they are focused in the forward direction in the laboratory frame, they can be identified in nuclear charge (Z) and mass (A), with energy loss and time of flight measurements at a given magnetic rigidity. Recoil properties of the fragments are also determined (see below). A scan of magnetic rigidity leads to determination of the cross section of all produced isotopes. For a complete description of the experimental method, see [5, 6, 7].

For the first time, the production cross sections of all spallation residues have been determined down to 0.01mb for several systems. Each experiment has then led to the determination of several hundreds of isotopes production cross sections. The accuracy is better than 15%. Due to the in-flight analysis, all nuclei produced are identified before their radioactive decay and idependently of their chemical properties.

2.2 Kinetic energies

The velocity of each recoil fragment has been measured in the beam direction. From this, a mean value and a distribution width of kinetic energy in the center of mass have been extracted for each isotope. In the case of fragmentation, results agree within a few percent with Morrissey systematics [8].

Kinematic properties of fission fragments are very different from properties of fragmentation residues, because of the fission energy [6, 7]. Fission and fragmentation regimes are then clearly distinguished.

Fragments recoil properties are needed to estimate atom displacements. While this is not a very important concern for the target design, this point is of primary importance for the study of the accelerator window.

2.3 Production cross sections results

Full fragments isotopic distributions have already been determined for several systems by our collaboration: (Au+p) at 800 AMeV [5, 6], (U+p) at 1 AGeV [10], (U+d) at 1 AGeV [9], (Pb+p) at 1 AGeV [7], (Pb+d) at 1 AGeV [11]. (Pb+p) at 500 AMeV, (Fe+p, Fe+d) at 1 AGeV, 500 and 300 AMeV have been measured and are currently analyzed.

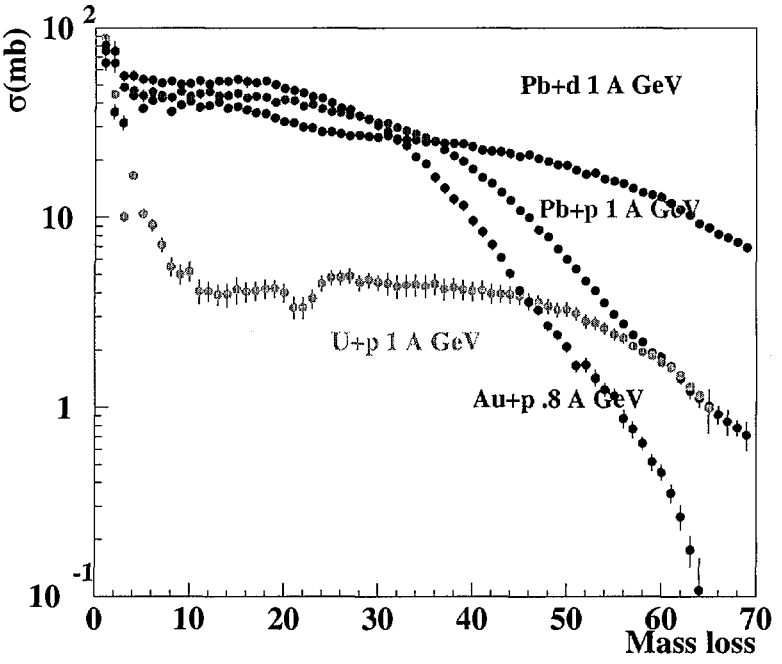

Figure 2: *Production cross section as a function of the mass loss with respect to the projectile, measured with inverse kinematics method for projectile fragmentation in systems Au+p at 800 AMeV, Pb+p at 1 AGeV, Pb+d at 1 AGeV, U+p at 1 AGeV. Fission is not included.*

Cross section distributions of fragmentation residues with respect to nuclear mass loss, are displayed in fig. 2. The smooth shape of the distributions is an evidence of the self-consistency of the measurements. The calculated total cross section for Au and Pb systems, obtained by summation of all production cross sections, agree with systematics [12] and other experiments within a few percent. Systematic comparison with previous data on gold from [2] also show an excellent agreement on the average [13].

Fragmentation cross sections of Au and Pb on protons show very similar shapes, with a slight shift toward large mass losses for Pb. This is a direct consequence of the higher projectile energy (800 AMeV for Au, 1 AGeV for Pb), which results in a higher mean deposited energy. This feature is confirmed by the results of Pb on d system at 1 AGeV, which exhibits even higher yield for larger mass losses. Furthermore in this system collisions are more violent: the energy is deposited by two nucleons instead of one, which increases the amount of thermalized energy.

The U curve exhibits a shape very different from the 3 other ones. The lower production cross sections for fragmentation residues is a direct consequence of the fission channel [10], which is favoured for U itself and for very heavy proton rich nuclei, populated by the evaporation process. Influence of the neutron shell closure at N=126 is responsible for the little drop in the curve around mass losses of 20: pre-actinides fragments formed by evaporation with 128 neutrons have a half-life close to the time of flight in the FRS. They partly decay by α-emission during their flight, and are then rejected by our analysis.

3 Results on lead and comparison with models

For the purpose of thick target simulation, isotopic cross sections calculations are a necessary first step. Several codes have been developped over the last thirty years, which are based on the spallation model first proposed by Serber [14]: a two step process consisting of a fast nucleon-nucleon collision phase (intranuclear cascade) followed by the decay of the thermally excited nuclei (evaporation). There are experimental evidences of an intermediate step called pre-equilibrium [15], but the improvement brought by inserting such a step in calculations highly depends on the caracteristics of the intranuclear cascade. We will come back on this point in the conclusion.

3.1 Mass distributions

Figure 3 displays complete distribution of cross sections of mass residues for Pb+p collisions at 1 AGeV [7]. One can easily distinguish the fragmention residues (down to A=130) from the bump of fission products centered at A=90. Note the large cross section measured for masses very close to the projectile.

Data are compared with distributions calculated obtained by several combinations of cascade and evaporation Monte-Carlo codes: Isabel[16]+ABLA[17], INCL[18]+ABLA, Bertini[19]+Dressner[20]. Gross features are reproduced by codes, but strong discrepancies show up.

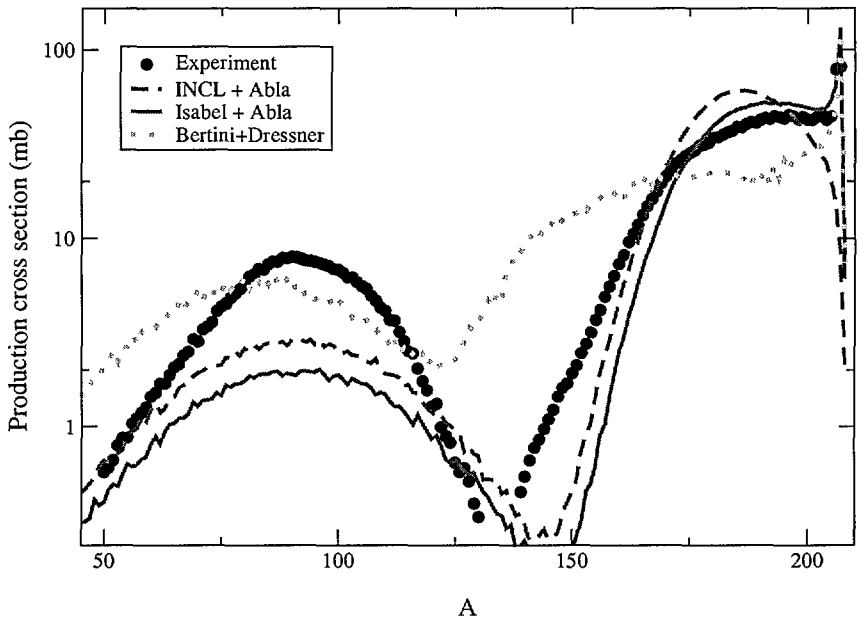

Figure 3: *Production cross section as a fonction of the mass of the residue in the H+Pb at 1 GeV reaction, from experimental data and from Monte-Carlo simulation codes.*

Fragments very close to the projectile (A<200) are produced by poorly excited prefragments originating from very peripheral collisions. Coupled with ABLA, Isabel reproduces fairly well the fragments distribution close to the projectile, while INCL fails. This can be explained by the too simple treatment of the nuclear surface by INCL: the nuclear density is approximated by a sharp step fonction. This problem is assumed to have been corrected in the very last version of INCL. The LAHET code, i.e. the Bertini cascade associated with Dressner evaporation code, shows a correct shape in this mass region but strongly underestimates production of fragments for mass losses superior to 4.

Both INCL+Abla and Isabel+Abla codes underestimates mass loss beyond 40. This tends to indicate that both cascade codes underestimate the high excitation energy tail of the excitation energy deposited during the collision. The opposite is true for LAHET and so it probably overestimates excitation energy. This assumption is confirmed by neutron production, which gives an estimation of the excitation energy, and is strongly overestimated by the LAHET code [15]. The large discrepancy between estimations from excitation energy by INCL and Bertini has also been studied in [21].

Fission probability is overall underestimated by a factor 3 to 4 by INCL+Abla and Isabel+Abla. The fission probability is only taken into account during the evaporation process, so this discrepancy indicates a failure from the evaporation code. The Bertini+Dressner code reproduces the global fission probability, but the fission product distribution is shifted toward low masses. This is coherent with an overestimation of the mean excitation energy.

3.2 Isotopic cross section distributions

Isotopic cross sections were measured for each element. The distributions, shown in fig 4, are centered on proton rich nuclei. They exhibit typical asymetric shapes with a slow fall on the neutron rich side and a fast fall on the proton rich side.

Those distributions, compared with results of simulation, help to discriminate between the influence of the cascade phase and the evaporation. In heavy nuclei, due to barrier suffered by charged particles, neutron emission is highly favoured in the deexcitation process, driving the nuclei to a region of the nuclear chart midway between the stable nuclei line and the proton dripline, called residues corridor.

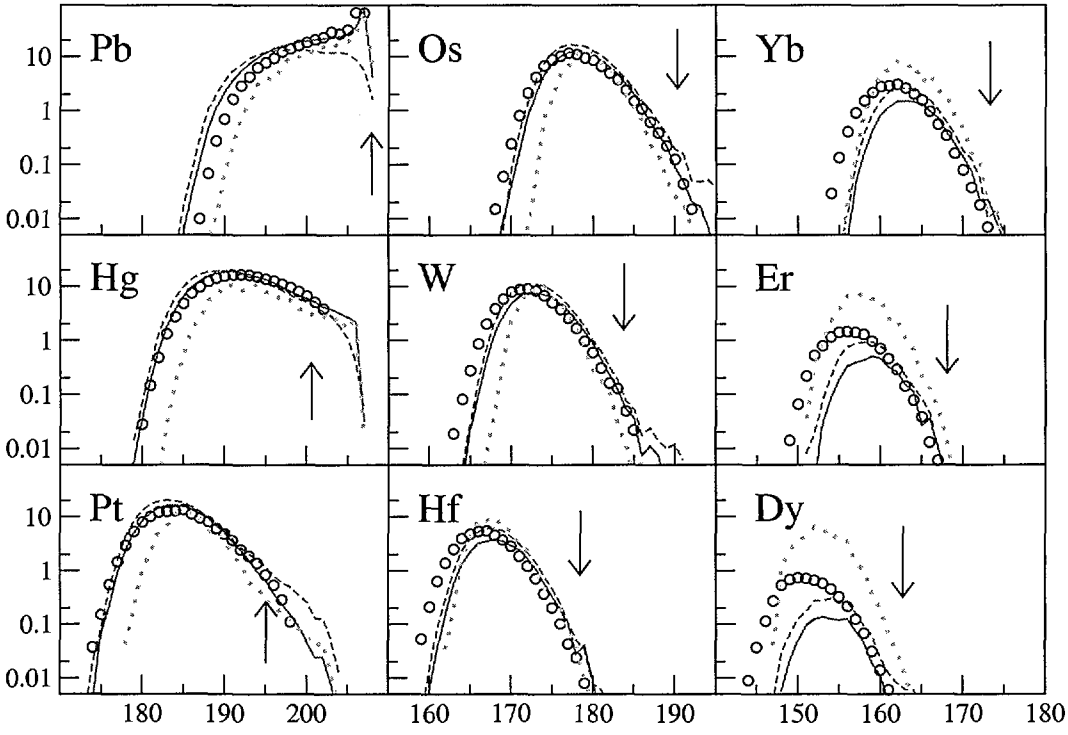

Figure 4: *Fragmentation residues production cross section as a fonction of the mass for even Z values between 66 and 82 in the H+Pb at 1 GeV reaction. Experimental data are plotted as circles. Lines represents codes calculations: Isabel+ABLA (continuous line), INCL+ABLA (discontinuous line), LAHET (crosses). Vertical arrows indicate mean mass of stable isotopes.*

In fig 4, one can see that Isabel+ABLA reproduces quite well the residues distribution in a range of 10 charge-units loss by the projectile. INCL+ABLA agrees well too, with the exception of the fragments very close to the projectile, as explained above. This is a clear sign of the quality of the ABLA code.

Bertini+Dressner underestimates the proton rich residues production. This effect does not depend on the element, so neither does it depend on the excitation energy. It indicates a failure from the Dressner evaporation code, related to Coulomb barriers evolution with excitation energy.

With decreasing Z, the fragment production is more and more underestimated by Isabel+ABLA and INCL+ABLA. This is consistent with the shape of the integrated mass distribution, and is an indication for an underestimation of high excitation energy events. The opposite is true for Bertini+Dressner. But one can also see that proton rich residue production is specifically more and more underestimated. If the evaporation step was correct, experimental results and calculations should be centered at the same

values. The discrepancy observed should come from the evaporation. The underestimation of α emission (pointed out in [10]) may be an explanation; evolution of barriers with excitation energy may also be considered.

3.3 Variation with projectile energy

In the spallation process, the intranuclear cascade is responsible for the emission of fast particles, mainly individual nucleons. It also sets the amount of energy left in the nucleus prior to evaporation. In a thick target, emitted fast particles produce new spallation reactions, thus propagating an internuclear cascade. The spallation reactions induced in this chain spans the whole range of projectile energy from nominal beam energy down to a few MeV. It is therefore necessary to predict individual residue production variations with energy.

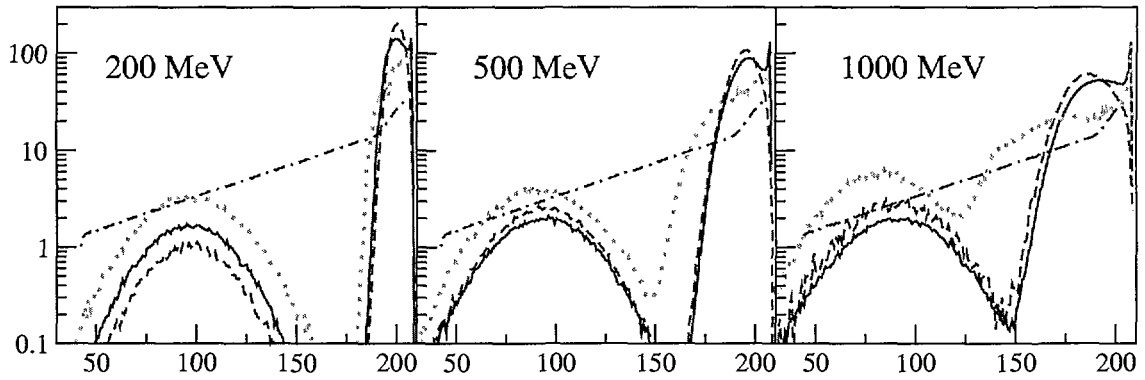

Figure 5: *Residues production cross section predictions as a fonction of the mass for projectile energies 200 MeV, 500 MeV and 1 GeV (left to right) in the H+Pb reaction. Green discontinuous line, violet continous line, orange dotted line the red dotted-dashed line represent respectively calculations by INCL+ABLA, Isabel+ABLA, Bertini+Dressner and EPAX.*

Fig 5 displays the mass distribution for incident projectile energy of 200, 500 and 1000 MeV as predicted by the same codes as the ones used above. Although one knows that agreement with data is far from being perfect, such calculations are reliable as long as only qualitative features are considered.

One can see that with the increasing energy, the fragmentation peak becomes broader, and finally joins the fission peak. This is the direct consequence of the increasing available excitation energy: as the prefragment excitation energy becomes higher, it evaporates more and more particles, and so, fragments further from the projectile are more and more favoured. This evolution is consistent with fig 3 as discussed above. Furthermore radiochemical measurements on a gold target on a broader energy range show a similar evolution with energy [2].

Fission probability slowly increases with incident energy. The excitation energy increases the prefragment probability of overcoming the fission barrier; but fission competes with particle emission, which is also favored by high excitation energy. Those two tendancies more or less compensate each other.

Calculations made with the widely used, semi-empirical EPAX [22] parametrization are also displayed. They do not depend on the projectile energy. Although they do not reproduce the data at all, they make sense because they represent the so-called fragmentation limit. This limit corresponds to the saturation of the excitation energy when one increases the projectile incident energy. For proton-induced collisions, this regime is known to be reached around 3 GeV. The evolution of the shape of the residues distribution with increasing energy toward such a shape is clearly visible in [2]. Note that EPAX does not take into account the fission process.

4 Toward a thick target simulation ?

The simulation of a thick target is our ultimate goal. First of all, there are still improvements to bring on spallation codes in order to obtain a good agreement with measured data. Even for the weakly

produced residues, there is a strong need for reliable estimation, as a few chemical elements are considered to be very harmful for materials even in very low quantities.

The target simulation requires prediction of reactions only on lead (and maybe other heavy metals such as bismuth). Note that gross features of the spallation physics are already understood and described: all Monte-Carlo codes considered here have no free parameters. INCL and ABLA are in constant developpement based on new insights in physics, so one can expect serious improvements in a near future. Nevertheless, we feel that new physics phenomena must be introduced in codes only if they offer real improvement in the codes. This is the reason why we do not consider pre-equilibrium: although it slighty increases LAHET predictions accordance with data, it has the opposite effect on INCL- or Isabel-based codes.

If very fine adjustement of the Monte-Carlo codes is not possible with physical arguments, it may then be valuable to develop semi-empirical parametrizations based on the Monte-Carlo calculations and fitting the data measured in a broad range of energy in the closest possible way.

All our results are in the process of being inserted in international databases, in collaboration with the NEA.

Once the differents reactions are completly described, the second step will be the transport of the particles and the decay of residues. Thick target simulation is the ultimate test for microscopic spallation model, because this tests the code ability to reproduce both residues and high and medium energy particle emissions. The transport shall not be an error source by itself; but it will certainly point out microscopic models deficiencies. Widely used, reliable codes such as GEANT [24] or MCNP [23] can be used as transport code, as long as total nuclear reaction cross section have been calculated with the microscopic code.

5 Conclusions

Full isotopic distributions of spallation residues produced in thin target have been measured for the first time, for several systems and at different relativistic energies, independently from their life time and from their chemical properties in inverse kinematics at FRS. Those measurement are of primary interest for the design of ADS, as they are needed to predict the evolution of the spallation target with time (induced radiotoxicity, cell corrosion, heating).

With respect to those exclusive data, a detailed comparison with several spallation codes has been made. It is concluded that although gross features are well described, no code is reliable enough to be used in a thick target simulation at the moment. Nevertheless, improvements in Monte-Carlo codes are expected in a near future, and a parametrization work is scheduled in order to bring a reliable tool for thick target simulation.

References

[1] S. Andriamonje et al. - Physics Letters B 348 (1995) 697.

[2] R. Michel et al. - Nuclear Instruments and Methods B 129 (1997) 153.

[3] Y.E. Titarenko et al. - Nuclear Instruments and Methods A 414 (1998) 73.

[4] H. Geissel, P. Armbruster et al. - Nuclear Instruments and Methods B 70 (1992) 286.

[5] F. Rejmund, B. Mustapha et al. - Nuclear Physics A 683 (2001) 540.

[6] J. Benlliure et al. - Nuclear Physics A 683 (2001) 513.

[7] T. Enqvist, W. Wlazlo et al. - Nuclear Physics A 686 (2001) 481.

[8] D.J. Morrissey - Physical Review C 39 (1989) 460.

[9] E. Casajeros et al., 5th International Conference on RNB, April 2000, Divonne, France - to be published in Nuclear Physics A Proceedings.

[10] J. Taieb - PhD Thesis, IPNO-T00-10.

[11] T. Enqvist et al. - to be submitted.

[12] R.E. Prael, M.B. Chadwick - International Conference on Nuclear Data for Science and Technology, Trieste, 1997

[13] B. Mustapha - PhD Thesis, IPNO-T99-05.

[14] R. Serber - Physical Review 72 (1947) 1114.

[15] M. Enke - Nuclear Physics A 657 (1999) 317.

[16] Y. Yariv, Z. Frankel - Physical Review C 20 (1979) 2227.

[17] A.R. Junghans, M. DeJong, H.-G. Clerc, A.V. Igniatyuk, G.A. Kudyaev, K.-H. Schmidt - Nuclear Physics A 629 (1998) 635.

[18] J. Cugnon, C. Volant, S. Vuillier - Nuclear Physics A 620 (1997) 475.

[19] H.W. Bertini - Physical Review 188 (1969) 1711.

[20] L. Dressner - Oak Ridge National Laboratory Report ORNL-TM-196 (1962).

[21] Cecile Toccoli - PhD Thesis, IPNO-T00.

[22] K. Summerer, B. Blank - Physical Review C 61 (2000) 346.

[23] Judith F. Briesmeister (editor) - "MCNP, A General Monte Carlo N-Particle Transport Code", Los Alamos National Laboratory report LA-13709-M.

[24] J. Apostolakis for the Geant4 Collaboration - "An Overview of Geant4's Production Release", World Scientific (1999).